

HYDRIDE FORMATION IN CHOSEN LANISN ALLOYS

¹Lubomír KRÁL, ¹Ondřej ZOBAČ, ¹Sanjay ULLATTIL, ¹Pavla ROUPCOVÁ, ²Michal ZYM, ²Bedřich SMETANA, ^{3,4}Merkur SMAJLAJ, ⁴Franz RENZ

¹ Institute of Physics of Materials CAS v.v.i., Brno, Czech Republic, EU, <u>lkral@ipm.cz</u>
 ²TUO - Technical University of Ostrava, Ostrava, Faculty of Materials Science and Technology, Department of Chemistry and Physico-Chemical Processes, Czech Republic, EU, <u>bedrich.smetana@vsb.cz</u>
 ³Hydrosolid GMBH, Wilhelmsburg, Austria, EU, <u>m.smajlaj@hydrosolid.com</u>
 ⁴LUH - Institute for Coordination Chemistry, Hannover, Germany, EU, <u>franz.renz@acd.uni-hannover.de</u>

https://doi.org/10.37904/metal.2025.5144

Abstract

The hydrogen storage properties of ball-milled AB_5 -type alloys containing La (a rare earth element) and Ni, Sn were investigated in this study. The experimental alloys were prepared using a compact arc melter under a high-purity argon atmosphere (99.9999%). The influence of microstructure and phase composition on the hydrogen absorption and desorption behavior was examined. The addition of Sn to the LaNi $_5$ intermetallic significantly reduced the equilibrium pressure without decreasing the maximum hydrogen absorption capacity, up to a Sn content of 10 wt%. Furthermore, increasing the Sn content enhanced the hydrogen absorption rate and slightly stabilized the hydride phase H_6LaNi_5 .

Keywords: Hydrides, LaNi5, hydrogen storage, LaNiSn alloys

1. INTRODUCTION

Metal hydrides, as multifunctional materials, are of particular importance for hydrogen-related technologies. In addition to their widespread use in nickel-metal hydride (Ni-MH) batteries and solid-state hydrogen storage systems, metal hydrides have demonstrated effectiveness in thermosorption compression, heat pumps, sensors, getters, and hydrogen separation and purification applications [1]. The use of solid hydrogen storage materials (HSMs) is among the most technologically promising approaches for hydrogen storage (HS). A wide range of compounds are currently under investigation for this purpose, including intermetallic hydrides (e.g., AB₂, AB₅), magnesium hydrides (MH₂), complex hydrides (e.g., alanates, borohydrides), chemical hydrides (e.g., amides, aminoboranes), multicomponent alloys (e.g., high-entropy alloys (HEAs), medium-entropy alloys (MEAs)), and adsorbent materials (e.g., nanocarbons, metal-organic frameworks (MOFs)) [2-4]. However, none of these materials fully meet all the practical requirements for HS-namely, high hydrogen capacity, good reversibility, and low cost. For instance, the U.S. Department of Energy (DOE) target for portable hydrogen storage systems specifies a gravimetric hydrogen capacity of 4.5 wt% at moderate pressures and operating temperatures between 233-333 K [2]. This corresponds to an energy density of approximately 1.5 kWh/kg, substantially higher than the average energy density of current vehicle batteries (~0.25 kWh/kg) [5]. Therefore, the investigation of materials with hydrogen storage capacities below 4.5 wt% remains meaningful and relevant. In particular, metal hydrides with gravimetric capacities of ≥1 wt% at moderate pressures (~1 MPa) and temperatures (253–373 K) offer a promising direction for practical HS applications [6–7]. Among these, AB_s-type LaNi_s-based intermetallics (where A is a rare earth element and B is a transition or p-block element) have attracted considerable attention due to their favorable hydrogen sorption kinetics and thermodynamics [8–10]. These materials can absorb and desorb hydrogen at relatively low equilibrium pressures (<1 MPa) and moderate temperatures (<373 K), making them suitable for integration with fuel cell systems [11]. Additionally,



they exhibit good activation behavior and oxidation resistance [12]. La–Ni–Sn-based alloys, derived from the AB₅-type LaNi₅ structure, are particularly promising for HS due to their reversible hydride formation and moderate operating conditions. This La–Ni–Sn system also contains a variety of intermetallic phases, making it a suitable model for studying the influence of different LaNiSn-based phases on hydrogen storage properties (**Figure 1**). Partial substitution of Ni by Sn modifies the electronic and crystallographic environment of the alloy, influencing hydrogen absorption and desorption behavior. Sn substitution typically reduces the equilibrium plateau pressure and enhances the thermal and structural stability of the hydride during cycling [13, 14]. It also suppresses the formation of undesired secondary phases and mitigates degradation mechanisms such as disproportionation and pulverization, thereby improving cyclic stability [15]. However, an excessive Sn content can reduce hydrogen storage capacity, as Sn has a weaker affinity for hydrogen compared to Ni. Thus, optimizing the Sn content is crucial to maintaining the CaCu₅-type structure and achieving favorable hydrogen sorption kinetics and thermodynamics [16-17].

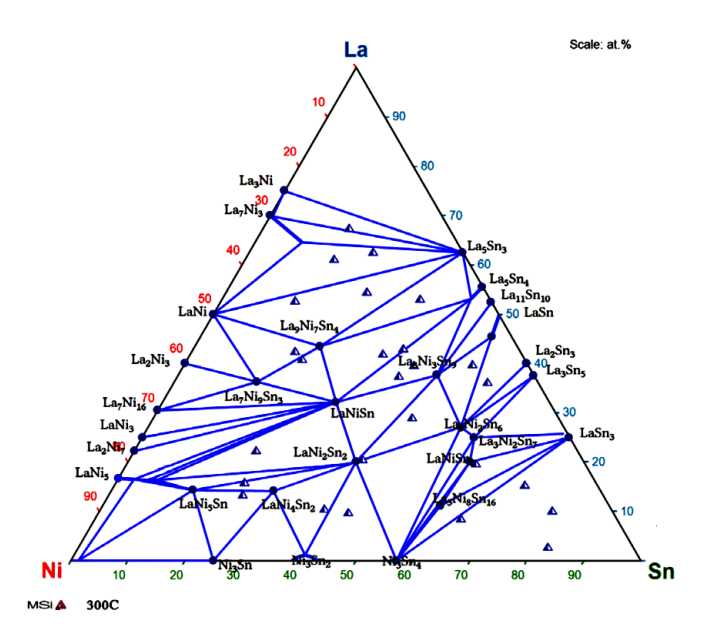


Figure 1 Phase diagram LaNiSn at 573K [18]

2. EXPERIMENTAL

The experimental materials were prepared from high-purity elemental precursors: La, Ni, Sn (La 99.9%, Ni 99.99%, Sn 99.99%). LaNi-based alloys were synthesized by induction melting of the pure metals in an argon atmosphere, followed by casting into a copper crucible. The cast samples were further homogenized by remelting three times using a compact arc-melter (MAM-1) under high-purity argon (99.9999%). The resulting ingots were drop-shaped with approximate dimensions of 10 mm in diameter and 5 mm in height. The cast alloys were annealed at 823 K for 720 hours to reach equilibrium structure. To enhance the HS properties while maintaining the microstructure, the annealed samples were mechanically crushed in an agate mortar. The resulting powders were sieved (sieve mesh 0.063) to a particle size of ≤0.63 µm. Microstructural and chemical composition analyses were performed using a Tescan LYRA 3 XMU FEG/SEM×FIB scanning electron microscope equipped with an Oxford Instruments X-Max80 EDS detector and a Nordlys Nano EBSD detector. Hydrogen sorption kinetics and pressure-composition-temperature (PCT) isotherms were measured using a Sieverts-type gas sorption analyzer (PCT-PRO, Setaram Instrumentation). This fully automated system enables safe and reproducible measurements in both absorption and desorption modes using high-purity hydrogen gas (99.9999%). Approximately 150 mg of powder was used for each measurement. Prior to sorption testing, the reaction chamber was evacuated to a pressure of 3×10⁻⁴ MPa, and the samples were heated to the desired constant temperature (ranging from 273 to 328 K). Sorption experiments were conducted under



an initial hydrogen pressure of approximately 4.0 MPa for absorption and 5×10^{-4} MPa for desorption. Phase composition and crystal structure of the powders were analyzed by X-ray diffraction (XRD) using X'Pert Pro and Empyrean diffractometers with Co K $\alpha_{1,2}$ radiation. XRD pattern analysis was conducted using HighScore Plus 4 software equipped with the PDF-2 and ICSD databases. To characterize the hydride phases, XRD measurements were carried out at a low temperature (~278 K) due to the limited stability of the hydride phase under ambient conditions.

3. RESULTS AND DISCUSSION

3.1 Structure of experimental materials

The average chemical composition and phase distribution of the main elements and phases in the experimental powdered materials are summarized in **Table 1**. All experimental LaNi₅ based alloys had similar Ni contents, with the Sn content increasing from 0 to approximately 13 wt%. The chemical compositions of the La(Ni,Sn)₅ alloys have been chosen to lie between the hydride-forming LaNi₅ and the non-hydride-forming LaNiSn₅ phases.

 Table 1 Chemical composition of studied alloys and content of hydride forming phases

Alloy	Chemical composition (wt%)			Content of hydride-forming phases (%)	
	La	Ni	Sn	LaNi₅	LaNi _{0.7} Sn _{0.3}
LaNi ₅	33.2	66.8	-	100.0	
55Ni_Sn10	34.9	54.9	10.2	57.0	39.0
55Ni_Sn13	31.9	55.1	13.0	29.0	68.0

While Ni and La appeared to be homogeneously distributed in the alloys 55Ni_Sn10 and 55Ni_Sn13, Sn was observed to segregate into distinct strip-like regions. Due to the high affinity of La for oxygen, occasional La-oxide particles were also detected in the microstructure (**Figure 2**). Despite the use of high-purity protective atmospheres, complete prevention of La oxidation during arc melting was not possible.

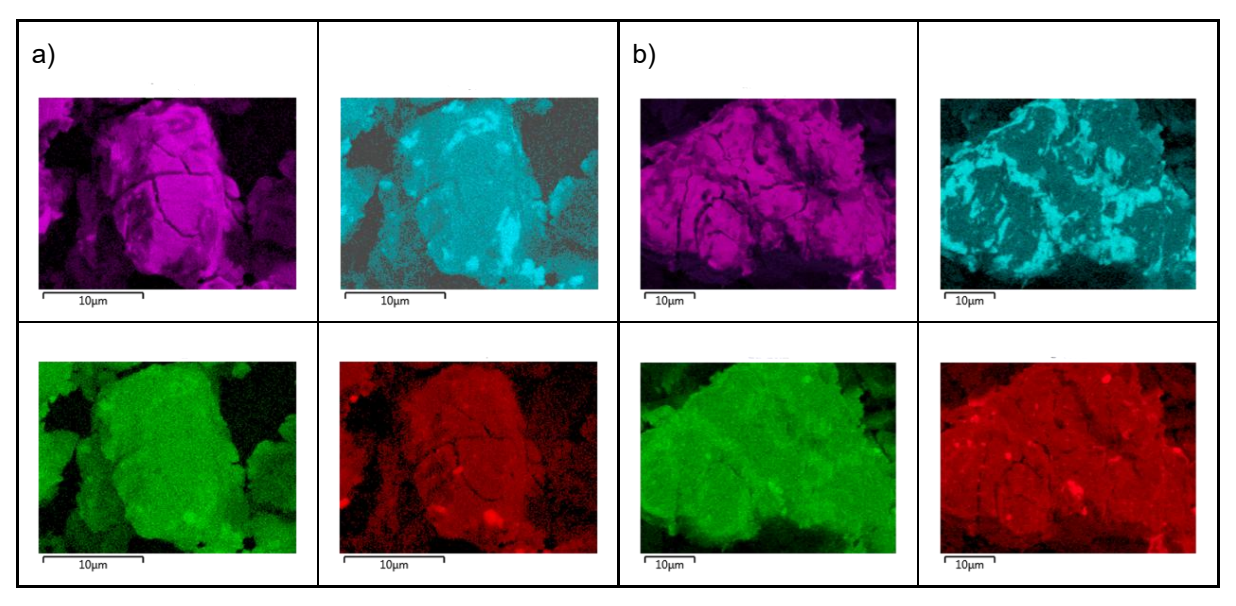


Figure 2 Chemical maps of studied alloys a) 55Ni_Sn10 and b) 55Ni_Sn13, Ni-violet, Sn-blue, Lagreen, O-red



The primary phases were identified via X-ray diffraction (XRD) analysis, and their contents in the studied alloys were quantified using Rietveld refinement (**Table 1**). Phase identification was supported by SEM-EDS analysis. Regions with lower Sn concentrations were identified as LaNi₅, while areas with higher Sn content corresponded to LaNi_{4.7}Sn_{0.3} (**Figure 2**). These LaNi₅-type phases were difficult to distinguish in the XRD patterns due to their similar diffraction peaks. However, an increasing presence of LaNi_{4.7}Sn_{0.3} caused a broadening and slight shift of the original LaNi₅ peaks toward lower diffraction angles, and in some cases, partial peak separation was observed (**Figure 3**). This shift indicates lattice expansion in LaNi_{4.7}Sn_{0.3} compared to LaNi₅. In addition to LaNi₅-type phases, the 55Ni_Sn10 and 55Ni_Sn13 alloys also contained phases such as H₂LaNiSn, LaNi₄Sn₂, and elemental Sn. The H₂LaNiSn phase was found to be stable after desorption, indicating incomplete hydrogen release, while LaNi₄Sn₂ and Sn do not form hydrides. It is evident that the LaNi₅-type phases formed the hydride H₆LaNi₅. Although partial hydrogen desorption occurred during XRD measurements, both LaNi₅ and LaNi_{4.7}Sn_{0.3} were confirmed to form H₆LaNi₅-type hydrides. It can be assumed that this type of hydride is formed from LaNi₅-type phases, which are not distinguished by XRD. This assumption is supported by the comparable hydrogen absorption capacities of 55Ni_Sn10 and LaNi₅ alloys (**Figure 4, 5**) and by the absence of Sn phase formation (**Figure 3**).

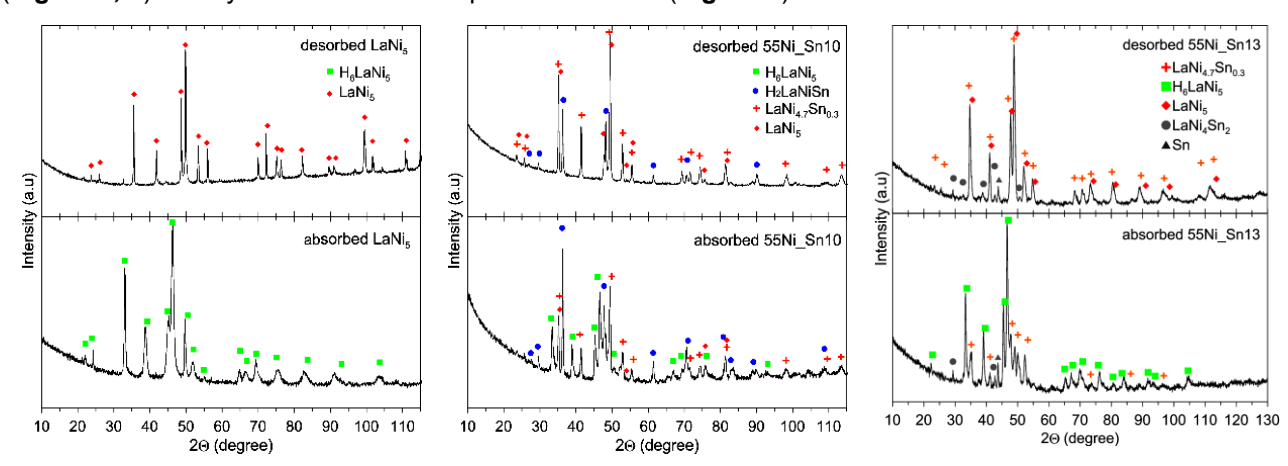


Figure 3 XRD patterns of studied alloys

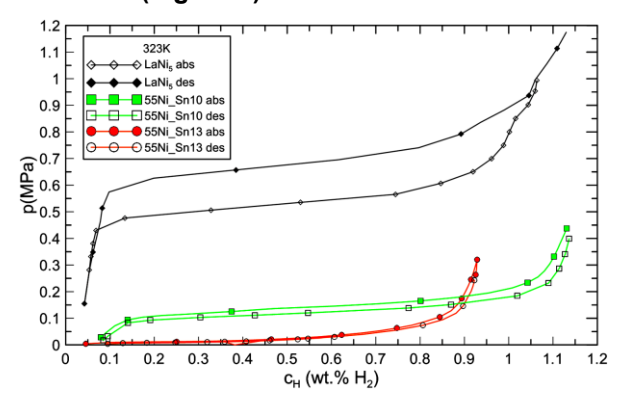
 Table 2 Thermodynamic properties of absorption/desorption

alloy	∆ <i>H</i> (kJ/mol) abs/des	∆ <i>H</i> (kJ/mol·K) abs/des	<i>p</i> _{abs} / <i>p</i> _{des} (MPa), 323K
LaNi₅	-30.5±0.8/33.5±1.3	129.3±2.6/135.9±4.2	0.69/0.51
55Ni_Sn10	-33.9± 0.4/33.4±0.6	126.7±1.1/124.8±1.7	0.14/0.13
55Ni_Sn13	-39.6± 2.3/40.9± 1.3	128.4±6.8/131.5±3.9	0.02/0.02

To evaluate the sorption behavior of the experimental materials, hydrogen absorption/desorption kinetics and pressure–composition–temperature (PCT) isotherms were measured. Measurements were conducted after three activation cycles at 323 K to ensure stable sorption properties. The maximum hydrogen concentration remained comparable to that of LaNi₅ for Sn contents up to 10 wt%. Beyond this point, a significant reduction in hydrogen capacity was observed (**Figure 4**), primarily due to the formation of non-hydride-forming phases such as Sn and LaNi₄Sn₂ (**Figure 3**). The addition of Sn also led to a decrease in the equilibrium pressures for both absorption (p_{abs}) and desorption (p_{des}), and reduced the pressure hysteresis (**Figure 4**). This behavior is likely attributed to the synergistic formation and decomposition of H₆LaNi₅-type hydrides derived from



LaNi_{4.7}Sn_{0.3} and LaNi₅ phases. A stronger effect on the equilibrium pressure was observed with increasing LaNi_{4.7}Sn_{0.3} content. The temperature dependence of the equilibrium pressure was used to construct Van't Hoff plots (**Figure 6**), from which the enthalpy (ΔH) and entropy (ΔS) of hydride formation/decomposition of H₆LaNi₅ were evaluated [17]. These thermodynamic parameters (**Table 2**) were consistent with those of LaNi₅ and previously reported values [17–20]. Notably, increasing the Sn content up to 13 wt% slightly stabilizes hydride H₆LaNi₅. However, hydrogen sorption kinetics was more strongly influenced by higher Sn content. The 55Ni_Sn10 and 55Ni_Sn13 alloys exhibited faster hydrogen absorption compared to LaNi₅ under similar conditions (**Figure 5**).



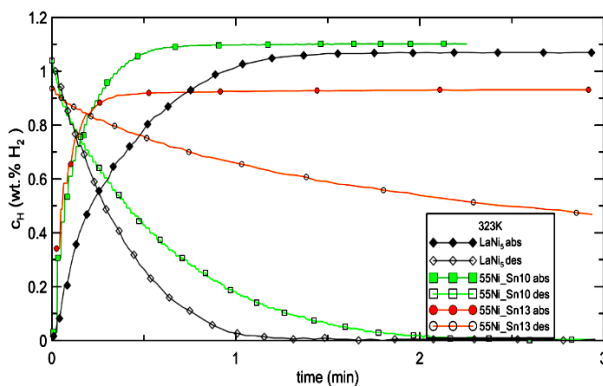


Figure 4 PCT plot of studied alloys

Figure 5 Kinetic curves of studied alloys

In contrast, desorption kinetic measurements were affected by starting pressures (\sim 0.03–0.04 MPa) that were too close to the $p_{\rm des}$ of 55Ni_Sn10 and 55Ni_Sn13, thereby slowing the release rate. In the case of 55Ni_Sn13, $p_{\rm des}$ was so low that complete hydrogen desorption could not be achieved under the given conditions.

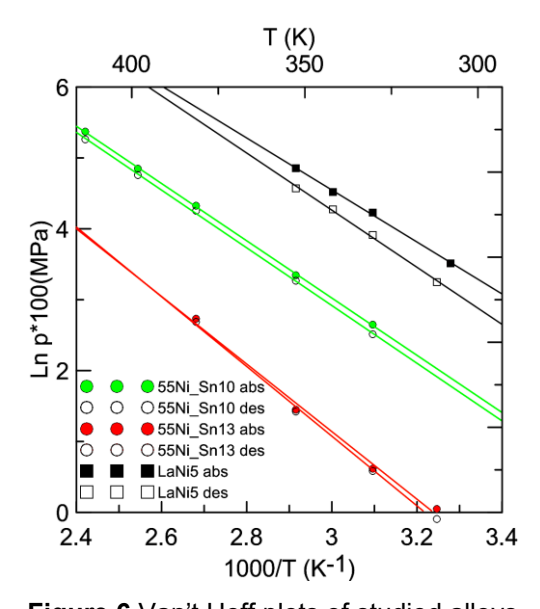


Figure 6 Van't Hoff plots of studied alloys

4. CONCLUSION

- 1. The addition of Sn into LaNi₅ intermetallic significantly decreased $p_{abs/p_{des}}$ of LaNi₅-based alloys and slightly stabilize hydride H₆LaNi₅.
- 2. The maximum capacity of H₂ in the LaNi₅-based alloys with content up to 10 wt% Sn is similar as in intermetallic LaNi₅. It is mainly caused by formation LaNi₅ phases, which form H₆LaNi₅ hydride.



- 3. Formation of non-hydride phases caused decreasing of maximum hydrogen concentration in studied LaNiSn alloys
- 4. The increasing content of Sn in LaNi₅-based alloys improved rate of absorbed hydrogen. However, the desorption rate of hydrogen decreased due to low p_{abs} of alloys 55Ni_Sn10 and 55Ni_Sn13.

ACKNOWLEDGEMENTS

This paper was created as part of the project No. CZ.02.01.01/00/22_008/0004631 Materials and technologies for sustainable development within the Jan Amos Komensky Operational Program financed by the European Union and from the state budget of the Czech Republic and the present paper was supported by the Institute of Physics of Materials AS CR, CZ-61662 Brno, Czech Republic, program Strategy AV21, program Sustainable energy; Project: Hydrogen technologies AV21/27.

Data Availability Statement: The data presented in study are available on Zenodo,

https://doi.org/10.5281/zenodo.15395389.

REFERENCES

- [1] KONIK, P., BERDONOSOVA, E., SAVVOTIN, I., et al. Structure and hydrogenation features of mechanically activated LaNi5-type alloys. *Int. J. Hydrogen Energy.* 2021, vol. 46, pp. 13638-13646.
- [2] RUSMAN, N.A.A., DAHARI, M.A. review on the current progress of metal hydrides material for solid-state hydrogen storage applications. *Int. J. Hydrogen Energy.* 2016, vol. 41, pp. 12108–12126.
- [3] CERMAK, J., KRAL, L., ROUPCOVA, P. Hydrogen storage in TiVCrMo and TiZrNbHf multiprinciple-element alloys and their catalytic effect upon hydrogen storage in Mg. *Renewable Energy*. 2022, vol.188, pp. 411–424.
- [4] ZELEŇÁK, V., SALDAN, I. Factors affecting hydrogen adsorption in metal–organic frameworks: A short review. *Nanomaterials*. 2021, vol. 11, pp. 1638.
- [5] CAO, W., ZHANG, J., LI, H. Batteries with high theoretical energy densities. *Energy Storage Mater.* 2020, vol. 26, pp. 46–55.
- [6] CASINI, J.C.S., SILVA, F.M., GUO, Z., LIU, H.K., FARIA, R.N., TAKIISHI, H. Effects of substituting Cu for Sn on the microstructure and hydrogen absorption properties of Co-free AB₅ alloys. *Int. J. Hydrogen Energy.* 2016, vol.41, pp. 17022–17028.
- [7] DING, N., LI, Y., LIANG, F., LIU, B., LIU, W., WANG, Q., WANG, L. Highly efficient hydrogen storage capacity of 2.5 wt % above 0.1 MPa using Y and Cr codoped V-based alloys. *ACS Appl. Energy Mater.* 2022, vol. 5, pp. 3282–3289.
- [8] JIANG, W., TAN, C., HUANG, J., OUYANG, L., CHEN, M., MIN, D., LIAO, C., TANG, R., ZHU, M. Influence of Sm doping on thermodynamics and electrochemical performance of AB_{5+z} alloys in low-temperature and high-power Ni-metal hydride batteries. *J. Power Sources*. 2021, vol. 493, pp. 229725.
- [9] TAN, C., OUYANG, L., MIN, D., LIAO, C., ZHU, M. A Nb-doped metal hydride electrode with overcharge resistance and wide temperature performance for aqueous rechargeable batteries. *Scr. Mater.* 2022, vol. 218, pp. 114827.
- [10] CHEN, P., ZHU, M. Recent progress in hydrogen storage. *Mater. Today.* 2008, vol. 11, pp. 36–43.
- [11] CHESALKIN, A., MARTAUS, A., AVERINA, J.M., MEN'SHIKOV, V.V. La–Ni based alloy modification by Ce and Fe for the next hydrogen storage in low-temperature metal hydrides. *Russ. J. Non-ferrous Metals*. 2019, vol.60, pp. 492–498.
- [12] NGUYEN, H. Q., SHABANI, B. Review of metal hydride hydrogen storage thermal management for use in the fuel cell systems. *Int. J. Hydrogen Energy.* 2021, vol. 46, pp. 31699–31726.
- [13] LIAO, B., LEI, Y.Q., CHEN, L.X., LU, G.L., PAN, H.G., WANG, Q.D. A study on the structure and electrochemical properties of La₂Mg(Ni_{0.95}M_{0.05})₉ (M = Co, Mn, Fe, Al, Cu, Sn) hydrogen storage electrode alloys. *J. Alloys Compd.* 2004, vol. 376, pp. 186-195.
- [14] XU, Y. et al. Enhanced cycling stability and reduced hysteresis of AB5-type hydrogen storage alloys by partial substitution of Sn for Ni. *Int. J. Hydrogen Energy*. 2022, vol. 44, pp. 6231–6237.
- [15] SIMIČIĆ, M.V., ZDUJIĆ, M., JELOVAC, D.M., RAKIN, P.M. Hydrogen storage material based on LaNi₅ alloy produced by mechanical alloying. *J. Power Sources*. 2001, vol. 92, pp. 250–254.



- [16] LUO, S., LUO, W., CLEWLEY, J.D., FLANAGAN, B.T., WADE, A. L. Thermodynamic studies of the LaNis_xSnx-H system from x = 0 to 0.5. *J. Alloys Compd.* 2002, vol. 231, pp.467–472.
- [17] CANTRELL, S.J., BEITER, A.T., BOWMAN, C.R. Crystal structure and hydriding behavior of LaNi_{5-y}Sn_y.*J. Alloys Compd.* 1994, vol. 207-208, pp. 372-376.
- [18] ZOBAČ, O., KRÁL, L., RICHTER, W.K., KROUPA, A. Experimental and theoretical study of La-Ni-Sn system as a perspective hydrogen storage material. In: 51st International Conference on Computer Coupling of Phase Diagrams and Thermochemistry. Mannheim: CALPHAD LI, 2024, pp. 102.
- [19] KRÁL, L., CHESALKIN, A., ČERMÁK, J., ROUPCOVÁ, P., PRUSOV, E. Influence of Fe on the hydrogen storage properties of LaCeNi alloys. *Langmuir*. 2023, vol. 39, pp. 6061-6068.
- [20] ŁODZIANA, Z., DĘBSKI, A., CIOS, G., BUDZIAK, A. Ternary LaNi_{4.75}M_{0.25} Hydrogen Storage Alloys: Surface Segregation, Hydrogen Sorption and Thermodynamic Stability. *Int. J. Hydrogen Energy*. 2019, vol. 44, pp. 1760–1773.